

Received August 19, 2020, accepted August 23, 2020, date of publication August 31, 2020, date of current version September 11, 2020.

Digital Object Identifier 10.1109/ACCESS.2020.3020297

Smooth Trajectory Generation for Predefined Path With Pseudo Spectral Method

KAI ZHAO^{1,2}, ZHONGJIAN KANG^{1,2,3}, AND XIAOBO GUO²

¹College of Control Science and Engineering, China University of Petroleum (East China), Qingdao 266580, China

²College of Computer Science and Information Engineering, Anyang Institute of Technology, Anyang 455000, China

³College of New Energy, China University of Petroleum (East China), Qingdao 266580, China

Corresponding author: Zhongjian Kang (kangzjzh@163.com)

This work was supported in part by the Young Key Teachers of Colleges and Universities in Henan Province under Grant 2016GGJS-151.


ABSTRACT In view of smooth trajectory generation for a 3-axis machine tool, many methods have been presented. Among them, the optimal control based method is increasingly concerned, because it is considered to be able to make full use of kinematic abilities of machine tools. Under the unified framework of optimal control, the feedrate can be adjusted flexibly by adding or removing axial constraints and tangential constraints. But the problem of smooth trajectory generation (PSTG) based on optimal control for a machine tool is not easily to be solved. In this article, to efficiently solve the PSTG, it is divided into two sub-problems: the problem of minimum time trajectory planning (PMTTP) and the pseudo problem of smooth trajectory generation (PPSTG). Since both sub-problems are convex, the existence of unique solutions can be guaranteed. Then, the PMTTP and the PPSTG are transformed into nonlinear programming (NLP) problems with radau-pseudo-spectral (RPM) method successively. Due to convexity, the two NLP problems can be efficiently solved with mature optimization methods. In addition, the RPM method allows two sub-problems to have different Legendre-Gauss-Radau (LGR) points, thereby further saving computational costs. Finally, three different predefined paths are employed to test the proposed method, and simulation results show the effectiveness of proposed method.

INDEX TERMS Trajectory planning, numerical solution, pseudo spectral method, optimal control.

I. INTRODUCTION

For computer numerical control (CNC) machining, a smooth trajectory can greatly reduce the vibration and wear of machine tools, and avoid the depression of workpiece surface. In the light of high speed machining, the cycle time must be shorten as much as possible, keeping smooth machining trajectory. Hence, the problem of smooth trajectory generation (PSTG) has been attracting extensive attention of many researchers.

For example, to improve manufacturing quality with industrial manipulator, a penalized least squares method is employed to smooth the planned trajectory [1]. Considering contour error reduction, a NURBS interpolator with feedrate scheduling (NIFS) is presented, which consists of two parts: pre-processing and real-time interpolation [2]. The NIFS adopted many techniques, such as curve fitting, mapping NURBS parameter into arc-length, curve feature

The associate editor coordinating the review of this manuscript and approving it for publication was Zheng Chen .

detection and so on. These technologies mainly aim at improving the smoothness of feedrate profile and processing efficiency. To implement NURBS interpolation algorithm on a platform with insufficient computing power, another real-time NURBS interpolator is designed for micro machine tool [3]. The interpolator fits the feedrate into a cubic spline with respect to time, considering the machine dynamics and chord error. In view of abrupt change of command feedrate, a smooth feedrate profile can also be generated based on Neuro-Fuzzy network [4]. It is assumed that the machining mission must be divided into several parts due to the capacity of NC system. So the interpolation algorithm must adjust the feedrate adaptively according to the spindle speed for each part. However, trajectories planned by the above methods are not time optimal.

In the field of robotics, a trajectory planning task can be implemented with many mature optimization methods [5]. It can be formulated as a time-energy optimization problem which is solved with iterative Linear Quadratic Regulator [6]. Then robots can follow the path based on specific controllers,

such as optimal observer based controller [7]. For CNC machining, time optimal trajectory planning can further improve the machining efficiency. For example, a corner blend method with B-spline is proposed to smooth linear paths [8]. With linear programming, time optimal feedrate is obtained, and then the cycle time is greatly reduced. Likewise, many other time optimal control methods are introduced into the trajectory planning for CNC machining by researchers [9]–[11]. To avoid large deviations from predefined parameter path, a jerk-limited trajectory planning scheme with phase plane method is presented [12]. The scheme can obtain near time-optimal feedrate by transforming jerk constraints into limits for the curvature of the phase-space velocity. In fact, time optimal control problems can also be solved with numerical methods, such as control vector parameterization (CVP) method [13].

In addition, the PSTG for a linear path can be also transformed into time optimal control problems. For example, the corner transition for a linear path is formulated as a time optimal control problem adhering to transition tolerance and kinematic constraints [14]. Then the time optimal transition curve is obtained through indirect method based on Pontryagin’s minimum principle. Later, another fitting method for linear paths based on optimal control is proposed, which can obtain time optimal fitted curve and feedrate profile simultaneously [15].

Hence, there is no doubt that the optimal control method can play a very important role in CNC machining. Moreover, the optimal control theory is the most natural framework for solving the motion planning problems [16]. It is because that the framework of optimal control has many advantages. For example, the axial or tangential kinematic constraints can be flexibly added or removed. Besides, some performance constraints, such as chord error and contour error, can be also easily considered simultaneously. Benefiting from the rapid growth of computational power, more and more methods can be employed to solve optimal control problems, such as dynamic programming methods, direct transcription methods, indirect methods, etc. One of them is the pseudo spectral method, which has been successfully applied both in practise and in theory. For obstacle avoidance, a novel efficient guidance algorithm is presented for Unmanned Aircraft Systems (UAS) based on the pseudo spectral method [17]. The algorithm can generate the optimal trajectory for a aircraft dynamics model with three degrees of freedom. Pseudo-spectral methods are also used in robot motion planning. For example, a gauss-pseudo-spectral (GPM) method is applied to generate an optimal path for a multi-steering tractor-trailer mobile robot (MSTTMR) [18]. However, there are few literatures about pseudo spectral methods applied for trajectory planning of machine tools.

In this article, the PSTG for CNC machining along a predefined tool path is formulated as an optimization problem. For simplicity, a 3-axis machine tool is taken for example. And then this optimization problem is transformed

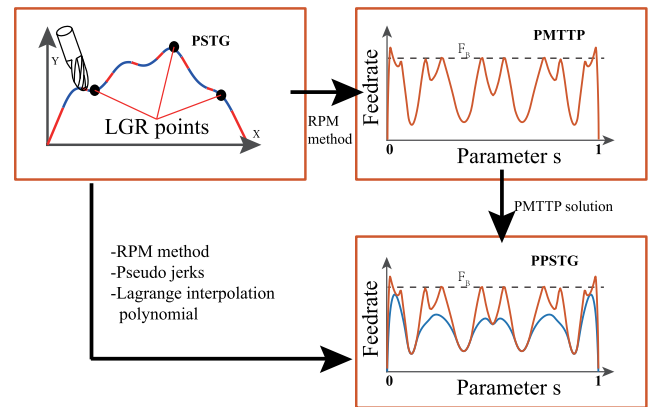


FIGURE 1. Structure of the proposed method.

into an optimal control problem by introducing the parameter of the tool path. In order to ensure machining accuracy, a convex optimal control scheme is constructed to obtain the unique solution based on radau-pseudo-spectral method. The main contribution of this article lies in two aspects. Firstly, we formulate non-convex PSTG as two convex optimal control subproblems, i.e. PMTTP and PPSTG, and introduce the radau-pseudo-spectral method to solve two sub-problems. Secondly, we derive the discrete form of PMTTP and PPSTG based on the LGR points. Then corresponding numerical solution algorithm is developed to efficiently obtain the solution. Fig. 1 summarizes the structure of our proposed method. The rest of the paper is organized as follows. In section II, the PSTG is addressed and formulated as an optimal control problem. Section III gives a detailed description of the proposed numerical solution algorithm. Simulation results are provided to illustrate the proposed method in section IV. Finally, conclusions are given in section V.

II. PROBLEM OF SMOOTH TRAJECTORY GENERATION

Let $\mathbf{C} = [x(s), y(s), z(s)]^T$ be a predefined path, which is a parametric curve where $s \in [0, 1]$. In order to finish machining a high-quality pattern in the shortest time, a tool tip should move along the predefined path according to an optimal smooth feedrate profile. Certainly, the motion is constrained by kinematic performances of the machine tool. Therefore, an optimization framework can be employed to express the problem of smooth trajectory generation (PSTG), which is formulated as

$$\begin{aligned} \min_{v, A_h, J_h} \quad & T = \int_0^{t_f} 1 dt \\ \text{s.t.} \quad & \begin{cases} 0 \leq v^2(t) \leq F_B^2 \\ -a_{h,B} \leq A_h(t) \leq a_{h,B} \\ -J_{h,B} \leq J_h(t) \leq J_{h,B} \end{cases} \end{aligned} \quad (1)$$

where $h \in \{x, y, z\}$ is the axis, $v(t)$ is the resultant feedrate, $A_h(t)$ is the axial acceleration, $J_h(t)$ is the axial jerk, and $F_B, a_{h,B}, J_{h,B}$ denote the corresponding bounds. Meanwhile,

some boundary conditions at start and final time must be satisfied, which can be written as

$$\begin{cases} v(0) = F_0, A_h(0) = a_{h,0}, \\ v(t_f) = F_{t_f}, A_h(t_f) = a_{h,t_f}. \end{cases} \quad (2)$$

However, constraints of the optimization problem composed of (1) and (2) are not explicit functions of time. Hence, it is difficult to obtain optimal solutions, especially $v(t)$. In order to simplify solving process, this optimization problem is transformed into an optimal control problem with fixed terminal time through introducing path parameter s . Let “ $'$ ” denote derivatives with respect to parameter s , and “ $\ddot{\cdot}$ ” denote derivatives with respect to time t . For example, assuming f is a function of time, such as feedrate, acceleration and jerk, there is $\frac{df}{dt} = \frac{df}{ds} \frac{ds}{dt} = f' \dot{s}$. Considering (2), the PSTG can be rewritten as

$$\begin{aligned} \min_{\dot{s}, \ddot{s}, \ddot{s}} \quad & T = \int_0^1 \frac{1}{\dot{s}} ds \\ \text{s.t.} \quad & \begin{cases} 0 \leq (x'^2 + y'^2 + z'^2) \dot{s}^2 \leq F_B^2 \\ -a_{h,B} \leq h' \ddot{s} + h'' \dot{s}^2 \leq a_{h,B} \\ -J_{h,B} \leq h' \ddot{\ddot{s}} + 3h'' \dot{s} \ddot{s} + h''' \dot{s}^3 \leq J_{h,B} \\ \dot{s}(0) = \dot{s}_0, \ddot{s}(0) = \ddot{s}_0 \\ \dot{s}(1) = \dot{s}_1, \ddot{s}(1) = \ddot{s}_1 \end{cases} \end{aligned} \quad (3)$$

where $\dot{s}_0 = \sqrt{\frac{F_0^2}{(x'^2+y'^2+z'^2)|_{s=0}}}$, $\ddot{s}_0 = \frac{a_{h,0}-h''\dot{s}_0^2}{h'}|_{s=0}$, $\dot{s}_1 = \sqrt{\frac{F_{t_f}^2}{(x'^2+y'^2+z'^2)|_{s=1}}}$ and $\ddot{s}_1 = \frac{a_{h,1}-h''\dot{s}_1^2}{h'}|_{s=0}$. Let $X = [\dot{s}, \ddot{s}]^T$ be the state vector, and $Y = \ddot{s}$ be the control variable. Then the system dynamics model is obtained as

$$\dot{X} = \begin{bmatrix} 0 & 1 \\ 0 & 0 \end{bmatrix} X + \begin{bmatrix} 0 \\ 1 \end{bmatrix} Y \quad (4)$$

The optimal control problem composed of (3) and (4) can not be efficiently solved, because it has a second order dynamics model and nonlinear constraints. In order to reduce the computational cost, new state and control variables are introduced [19], [20]. Define $m(s) = \dot{s}^2$, $u(s) = \ddot{s}$ as the new state variables, and let $v(s) = \frac{\ddot{s}}{\dot{s}}$ be the new control variable. According to the chain rule of differential, the new system dynamics model is expressed as

$$\begin{cases} m'(s) = 2\dot{s} \cdot \frac{d\dot{s}}{ds} = 2\dot{s} \cdot \frac{d\dot{s}}{dt} \frac{dt}{ds} = 2u(s) \\ u'(s) = \frac{d\ddot{s}}{ds} = \frac{d\ddot{s}}{dt} \frac{dt}{ds} = v(s) \end{cases} \quad (5)$$

Replace the state and control variables in (3) with new ones, the PSTG is reformulated again as

$$\min_{m,u,v} \quad T = \int_0^1 \frac{1}{\sqrt{m(s)}} ds \quad (6a)$$

$$\text{s.t.} \quad 0 \leq (x'^2 + y'^2 + z'^2)m(s) \leq F_B^2 \quad (6b)$$

$$-a_{h,B} \leq h'u(s) + h''m(s) \leq a_{h,B} \quad (6c)$$

$$-J_{h,B} \leq \sqrt{m(s)}\Gamma(s) \leq J_{h,B} \quad (6d)$$

$$m(0) = m_0, u(0) = u_0 \quad (6e)$$

$$m(1) = m_1, u(1) = u_1 \quad (6f)$$

$$m(s) > 0, s \in [0, 1] \quad (6g)$$

where $m_0 = \dot{s}_0^2$, $m_1 = \dot{s}_1^2$, $u_0 = \ddot{s}_0$, $u_1 = \ddot{s}_1$, and $\Gamma(s) = h'v(s) + 3h''u(s) + h'''m(s)$, $h \in [x, y, z]$. The feedrate constraint is expressed as (6b), and (6c) denotes the axial acceleration constraints. The transformation weakens the nonlinear path constraints. After conversion, the feedrate and axial acceleration constraints have become linear ones, which can greatly improve the efficiency of the solution. Moreover, the transformed objective function (6a) remains convex, which will be helpful for the subsequent numerical solution. The constraint (6d) denotes the real constraint for each axial jerk, and it will be replaced by a pseudo constraint in the next section to reduce computational cost. Generally, the optimal control problem represented by (5) and (6) is known as the nominal problem of smooth trajectory generation (NPSTG).

III. PROPOSED METHOD

A. PROBLEM OF CONVEX OPTIMAL CONTROL

Although the PSTG has been formulated as the NPSTG, it is still difficult to be solved because (6d) is a nonlinear path constraint, consisting of state and control variables. Furthermore, the NPSTG has non-convex feasible domain, which means the solution is not unique. For CNC system, non-unique solutions will lead to uncertain machining results. This is unacceptable in high precision machining. In this subsection, to overcome the drawback, a convex optimal control problem with a unique solution is constructed.

Note that the NPSTG is non-convex mainly because of (6d). Therefore, if the constraint range of (6d) is relaxed to $[-\infty, +\infty]$, the NPSTG will degenerated to the following problem of minimal time trajectory planning (PMTTP)

$$\min_{m,u,v} \quad T = \int_0^1 \frac{1}{\sqrt{m(s)}} ds \quad (7a)$$

$$\text{s.t.} \quad m(0) = m_0, u(0) = u_0, m(1) = m_1, u(1) = u_1 \quad (7b)$$

$$\begin{cases} m'(s) = 2u(s) \\ u'(s) = v(s) \end{cases} \quad (7c)$$

$$\begin{cases} 0 \leq (x'^2 + y'^2 + z'^2)m(s) \leq F_B^2 \\ -a_{h,B} \leq h'u(s) + h''m(s) \leq a_{h,B} \\ m(s) > 0, s \in [0, 1] \end{cases} \quad (7d)$$

The PMTTP is a typical convex optimal control problem, which can be solved more easily than the NPSTG. In addition, since the problem is convex, a unique solution exists. Moreover, there are some useful properties for PMTTP. For example, Zhang *et al.* [21] gave three properties of PMTTP for robotic manipulators. Regarding to the PMTTP for machine tools, Dong *et al.* [22] elaborated the necessary condition for optimality which is known as the “bang-bang” structures of control variables and constraints. Later, Zhang *et al.* [23] proved the “bang-bang” structures of constraints based on the extended maximum principle.

According to conclusions in the literatures mentioned above, the solution of PMTTP is maximum among all the feasible solutions. Although (7) is a little different with problems in literatures mentioned above, we could still infer that the first state variable $m(s)$ has the following feature,

$$m^*(s) \geq m_f(s) \tag{8}$$

where $m^*(s)$ is the first state of the optimal solution of PMTTP, and $m_f(s)$ denotes the first state of any one feasible solution. Eq. (8) can be proved by contradiction:

Proof: Consider another feasible solution $m_e(s)$ of (7), not satisfying (8). Thus, there are following two cases.

1) Case 1:

$$m_e(s) > m^*(s), s \in [0, 1].$$

2) Case 2:

$$\begin{cases} m_e(s) > m^*(s), & s \in [s_a, s_b] \text{ and } [s_a, s_b] \subseteq [0, 1], \\ m_e(s) \leq m^*(s), & \text{others.} \end{cases}$$

Then we discuss the two cases one by one.

For case 1: If case 1 holds, $\frac{1}{m_e(s)} < \frac{1}{m^*(s)}$ can be obtained. It means that the cost function value can get smaller at $m_e(s)$ than at $m^*(s)$. This contradicts that $m^*(s)$ is the optimal solution.

For case 2: Assume that the solution of (7) is continuous. If case 2 holds, we can easily construct a feasible solution which satisfies,

$$m_c(s) = \begin{cases} m_e(s), & s \in [s_a, s_b], \\ m^*(s), & \text{others.} \end{cases}$$

We can easily conclude that $\frac{1}{m_c(s)} < \frac{1}{m^*(s)}$, which also contradicts that $m^*(s)$ is the optimal solution.

Hence, Eq. (8) is proved.

Actually, since (7) is obtained by relaxing the real axial jerk constraints of the NPSTG, the feasible domain of the NPSTG is obviously the subset of feasible region of the PMTTP. Assume that $m_n(s)$ is the first state of any one solution of the NPSTG, there is

$$m^*(s) \geq m_n(s) \tag{9}$$

Based on (8), the nonlinear path constraint (6)d can be relaxed as the following linear one

$$-J_{h,B} \leq \sqrt{m^*(s)}\Gamma(s) \leq J_{h,B} \tag{10}$$

This means (10) is an underestimation of (6)d. Furthermore, (6) can be approximated by following convex optimal control problem,

$$\begin{aligned} \min_{m,u,v} \quad & T = \int_0^1 \frac{1}{\sqrt{m(s)}} ds \\ \text{s.t.} \quad & m(0) = m_0, u(0) = u_0, m(1) = m_1, u(1) = u_1 \end{aligned} \tag{11a}$$

$$\begin{cases} m'(s) = 2u(s) \\ u'(s) = v(s) \end{cases} \tag{11b}$$

$$\begin{cases} 0 \leq (x'^2 + y'^2 + z'^2)m(s) \leq F_B^2 \\ -a_{h,B} \leq h'u(s) + h''m(s) \leq a_{h,B} \\ -J_{h,B} \leq \sqrt{m^*(s)}\Gamma(s) \leq J_{h,B} \\ m(s) > 0, s \in [0, 1] \end{cases} \tag{11c}$$

Since real axial jerk constraints are approximated with (10), this convex optimal control problem (11) is known as the pseudo problem of smooth trajectory generation (PPSTG). To illustrate validity of the constraint approximation, the following theorem is given.

Theorem 1: The optimal solution of the PPSTG is the feasible one of the NPSTG.

Proof: Since all the constraints of the two problem are the same except axial jerk constraints, to prove the theorem, we only need to verify whether the optimal solution of PPSTG satisfies the (6)d. Define that the optimal solution vector of PPSTG is $\mathbf{W}_p = [m_p, u_p, v_p]^T$. Then substitute \mathbf{W}_p into the third constraint of (11)d, there is

$$-\frac{J_{h,B}}{\sqrt{m^*(s)}} \leq (h'v_p + 3h''u_p + h'''m_p) \leq \frac{J_{h,B}}{\sqrt{m^*(s)}}$$

Define any one solution vector of NPSTG is $\mathbf{W}_n = [m_n, u_n, v_n]^T$. Then substitute \mathbf{W}_n into (6)d, there is

$$-\frac{J_{h,B}}{\sqrt{m_n}} \leq (h'v_n + 3h''u_n + h'''m_n) \leq \frac{J_{h,B}}{\sqrt{m_n}}$$

From (9), we have

$$-\frac{J_{h,B}}{\sqrt{m_n}} \leq -\frac{J_{h,B}}{\sqrt{m^*(s)}}, \frac{J_{h,B}}{\sqrt{m_n}} \geq \frac{J_{h,B}}{\sqrt{m^*(s)}}$$

Hence, \mathbf{W}_p also satisfies the (6)d, and the theorem is proved.

B. NUMERICAL SOLUTION BASED ON PSEUDO-SPECTRAL METHOD

How to gain the optimal solution of aforementioned problems is still a challenging task. At present, there are several approaches to solve aforementioned problems, such as dynamic programming methods, control vector parameterization methods, and pseudo-spectral methods, etc. In this section, the radau-pseudo-spectral (RPM) method is applied to discretize continuous-time optimal control. The collocation points are obtained from the roots of following equation,

$$P_K(\sigma) + P_{K-1}(\sigma) = 0$$

where $P_K(\sigma)$ is the k th-degree legendre polynomial. These collocation points are located in half open interval $[-1, 1)$ or $(-1, 1]$. The points lying in the former interval are known as Legendre-Gauss-Radau (LGR) points, while those lying in the latter are known as flipped LGR points. Here, the LGR points are adopted.

Note that the domain of parameter s is $[0, 1]$, whereas the LGR points lie in the interval $[-1, 1)$. Hence, the domain

[0, 1] needs to be mapped to [-1, 1] by following transformation

$$s = \frac{1}{2}\sigma + \frac{1}{2}, \sigma \in [-1, 1] \quad (12)$$

Define N LGR points as $\sigma_1 < \sigma_2 < \dots < \sigma_N$, with $\sigma_1 = -1$ and $\sigma_N < 1$. In addition, the state variables are also approximated at the terminal point $\sigma_{N+1} = 1$ besides LGR points [24].

In view of (7), let $\mathbf{M} = [M_1, M_2, \dots, M_N, M_{N+1}]^T$, $\mathbf{U} = [U_1, U_2, \dots, U_N, U_{N+1}]^T$ be the values of state variables at LGR points and the terminal point. Therefore, state variables can be approximated by polynomials below,

$$\begin{cases} m(\sigma) \approx \sum_{j=1}^{N+1} M_j L_j(\sigma) \\ u(\sigma) \approx \sum_{j=1}^{N+1} U_j L_j(\sigma) \end{cases} \quad (13a)$$

$$L_j(\sigma) = \prod_{\substack{k=1 \\ k \neq j}}^{N+1} \frac{\sigma - \sigma_k}{\sigma_j - \sigma_k}, j = 1, 2, \dots, N + 1 \quad (13b)$$

where $L_j(\sigma)$ is a basis function of the N th-degree lagrange polynomial. Differentiating two series in (13)a and evaluating the values at σ_i , there are

$$\begin{cases} m'(\sigma_i) \approx \sum_{j=1}^{N+1} M_j L'_j(\sigma_i) = \sum_{j=1}^{N+1} D_{ij} M_j = \mathbf{DM} \\ u'(\sigma_i) \approx \sum_{j=1}^{N+1} U_j L'_j(\sigma_i) = \sum_{j=1}^{N+1} D_{ij} U_j = \mathbf{DU} \\ D_{ij} = L'_j(\sigma_i) \end{cases} \quad (14)$$

where \mathbf{D} is a $N \times N + 1$ matrix, known as radau-pseudo-spectral differentiation matrix. Thus, the system dynamics model (7)c can be approximated with

$$\begin{cases} \mathbf{DM} = \frac{1}{2} \cdot 2 \cdot \mathbf{U}^N = \mathbf{U}^N \\ \mathbf{DU} = \frac{1}{2} \mathbf{V}^N \end{cases} \quad (15)$$

where $\mathbf{U}^N = [U_1, U_2, \dots, U_N]^T$, and $\mathbf{V}^N = [V_1, V_2, \dots, V_N]^T$ are the values of $u(\sigma)$ and $v(\sigma)$ at LGR points.

Besides the system dynamics model, the cost function, boundary conditions and path constraints should be approximated, too. Unlike system dynamics model, they are only evaluated at LGR points. Hence, the cost function can be written as

$$T = \int_0^1 \frac{1}{\sqrt{m(s)}} ds = \frac{1}{2} \int_{-1}^1 \frac{1}{\sqrt{m(\sigma)}} d\sigma \approx \sum_{j=1}^{N+1} \varpi_j \frac{1}{\sqrt{M_j}} \quad (16)$$

where ϖ_j is the quadrature coefficient corresponding to σ_j . In view of the boundary constraints, we have

$$M_1 = m_0, M_{N+1} = m_1, U_1 = u_0, U_{N+1} = u_1 \quad (17)$$

Since the path constraints are associated with the predefined curve, values of tool path at LGR points are also needed to be estimated. Substituting $\sigma_j \in \{\sigma_1, \sigma_2, \dots, \sigma_N\}$ into (12),

the corresponding $s_j \in \{s_1, s_2, \dots, s_N\}$ are obtained. Then feedrate constraints, axial acceleration constraints, and state constraints are evaluated as follows

$$\begin{cases} 0 \leq (x'^2(s_j) + y'^2(s_j) + z'^2(s_j))M_j \leq F_B^2 \\ -a_{h,B} \leq h'(s_j)U_j + h''(s_j)M_j \leq a_{h,B} \\ M_j > 0 \end{cases} \quad (18)$$

Until now, the PMTTP has been transformed into a NLP problem composed of (15), (16), (17), and (18). The NLP problem can be easily solved with mature methods. Then the time optimal solution can be obtained, e.g. \mathbf{M} and \mathbf{U} . Considering that the number of LGR points for PMTTP and PPSTG may be different, especially when the self-adaptive pseudo-spectral method is adopted, $m^*(s)$ should be interpolated according to

$$m^*(s) = m^*(\sigma) \approx \sum_{j=1}^{N+1} M_j^* L_j(\sigma) \quad (19)$$

where $j \in \{1, \dots, N + 1\}$ denotes the j -th LGR point when solve the PMTTP, and M_j^* is the corresponding state value.

Since the PPSTG is gained by adding axial jerk constraints to the PMMTP, we only give the discretization of axial jerk constraints as follows

$$-J_{h,B} \leq \sqrt{m^*(s_j)}\Omega_j \leq J_{h,B} \quad (20)$$

where $\Omega_j = h'(s_j)V_j + 3h''(s_j)U_j + h'''(s_j)M_j$, and $m^*(s)$ is obtained from (19).

To sum up, the PSTG is firstly approximated with two sub-problems, and then two sub-problems can be solved with RPM-based method. The detail numerical algorithm is expressed as follows:

- 1) Specifying N , construct discrete PMTTP represented as (15)-(18). Note that the number of discrete meshes can be determined with adaptive methods.
- 2) Solve the discrete PMTTP with mature nonlinear programming methods. Then the maximum state series M_j^* , ($j = 1, \dots, N + 1$) is obtained.
- 3) Continuous $m^*(s)$ is approximated with lagrange interpolation polynomial. It is because that PMTTP and PPSTG may adopt different number of discrete meshes.
- 4) Substituting $m^*(s)$ into (19) and (20), obtain final results by solving the discrete PPSTG formulated as (15)- (18) and (20).

IV. NUMERICAL EXAMPLES

In this section, three examples are chosen as tool paths to illustrate the proposed method. Optimal control problems in example I and example II are solved by GPOPS [25]–[28] which is a software based on the hp self-adaptive RPM. Please note that several parameters of the software are set as follows: “mesh.tolerance” is 10^{-4} , “mesh.iteration” is 20, and “auto-scale” is off. The rest of parameters can be set as default. To obtain the entire control of solution progress, the optimal control problems in example III are solved with program

written by ourselves. For simplicity, all boundary conditions in simulations are set as zero.

All examples are implemented under a Matlab environment installed on a PC with a 64-bit windows 7 operation system. The PC is equipped with AMD A8-6500 processor and 4GB memory. In addition, since real time interpolation is not considered in following numerical examples, all implementations of trajectory generation are off-line.

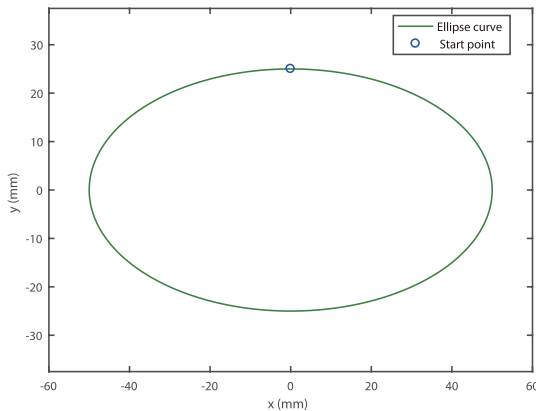


FIGURE 2. A ellipse pattern.

A. EXAMPLE I: A ELLIPSE PATH

The first predefined tool path is an ellipse curve shown as Fig.2. And the parametric expression of the ellipse is

$$C = [50\sin(2\pi s), 25\cos(2\pi s), 0.5]^T, s \in [0, 1] \quad (21)$$

For comparison, three kinds of optimal control problem, i.e., PMTTP, NPSTG and PPSTG, are all solved. Since the GPOPS can adjust the mesh adaptively, the final grids for PMTTP, NPSTG and PPSTG are 100, 1054 and 855 under the same precision requirement. The computation time for solving the three optimal control problems is 1.347s, 26.21s and 6.929s. To some extent, we can estimate the difficulty of solving three optimal control problems from the meshes and solution time. This further shows that the construction of convex optimization problem is necessary.

Fig.3 shows the feedrate profiles of PMTTP, NPSTG and PPSTG for the ellipse path. The feedrate bound is set as 100mm/s. In Fig.3, the feedrate profile of PMTTP is denoted with dashed line, and it fluctuates near the feedrate limit. It is because that there are no enough meshes for PMTTP. However, in our proposed method, solving PMTTP is only used to obtain the upper bound of the state. Therefore, a little fluctuation of feedrate profile of PMTTP is acceptable. Simulation results also verify the inference mentioned above. The feedrate profile of PPSTG is obtained based on the solution of PMTTP, which is indicated as the solid line. And it is completely bounded by feedrate limit and does not fluctuate at all. The dotted line shows feedrate profile of NPSTG which also has no fluctuations.

The acceleration profiles of three optimal control problems for the ellipse path are shown in Fig.4. Acceleration bounds

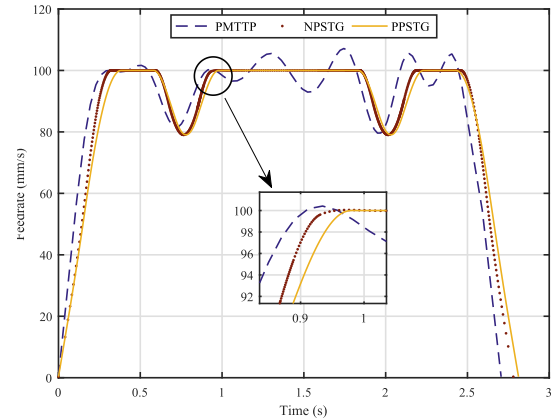


FIGURE 3. The feedrate profiles of PMTTP, NPSTG and PPSTG for the ellipse path.

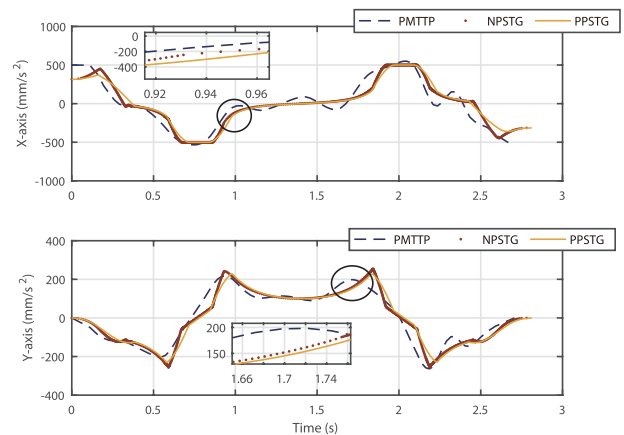


FIGURE 4. The axial acceleration profiles of PMTTP, NPSTG and PPSTG for the ellipse path.

for X-axis and Y-axis are both set as 500mm/s² in each problem. The profiles of PMTTP are denoted as dashed line, which changes frequently, especially on Y-axis. The profiles of NPSTG (dotted line) and PPSTG (solid line) become smoother than that of PMTTP, because jerk constraints play a role in two optimal control problems. From the plot of Y-axis, the acceleration planned by PPSTG is more smoother at some sharp corners than that planned by NPSTG.

Since the jerk constraints are not included in the PMTTP, only the jerk profiles of NPSTG and PPSTG are drawn in Fig.5. Jerk limits are set as 5000mm/s³ for two axes. Although the acceleration profiles are smoothed owing to the jerk constraints, the jerk itself on each axis has some fluctuations. From detail pictures, the jerk profiles of NPSTG show more violent fluctuations than that of PPSTG. In addition, the machining time of PMTTP, NPSTG and PPSTG are 2.705s, 2.780s, and 2.812s. The overall planning time of our proposed method is composed of the planning time of PMTTP and PPSTG, that is 8.276s. The planning time of proposed method is saved about 44% than that of NPSTG, whereas its machining time only extends 1.2%. Moreover, from the profiles of feedrate, acceleration and jerk presented in Figs.3-5, the structure of constraints are

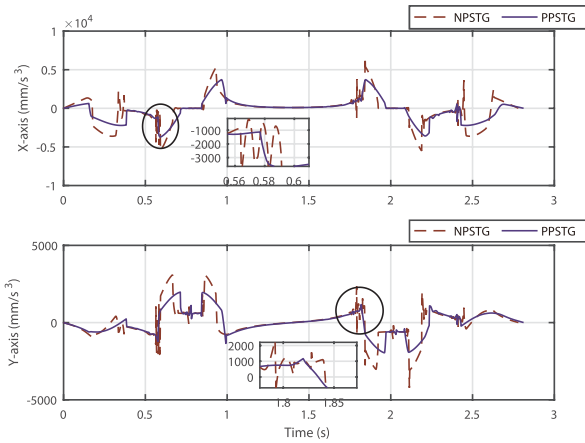


FIGURE 5. The axial jerk profiles of NPSTG and PPSTG for the ellipse path.

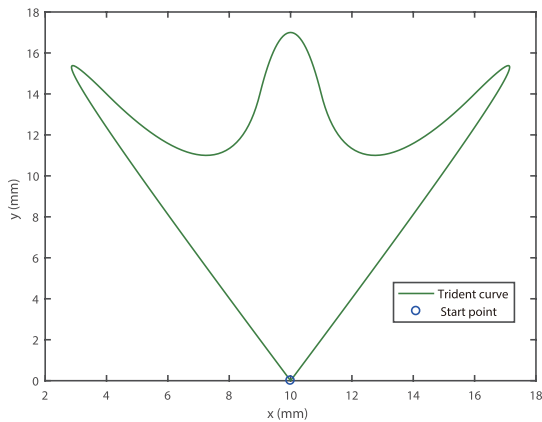


FIGURE 6. A trident pattern.

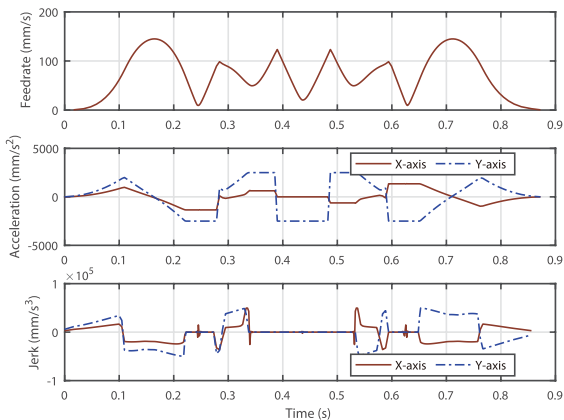


FIGURE 7. The profiles of feedrate, acceleration, jerk (the maximum jerk equals to 50000mm/s^3) for the trident path.

approximately “bang-bang” [21], which means at least one constraint reaches its bound throughout the motion. This verifies the reliability of the simulation results.

B. EXAMPLE II: A TRIDENT PATH

The parametric curves are widely used in modern machining industry, such as B-spline and NURBS curves. In this subsection, a NURBS curve of the trident shape shown

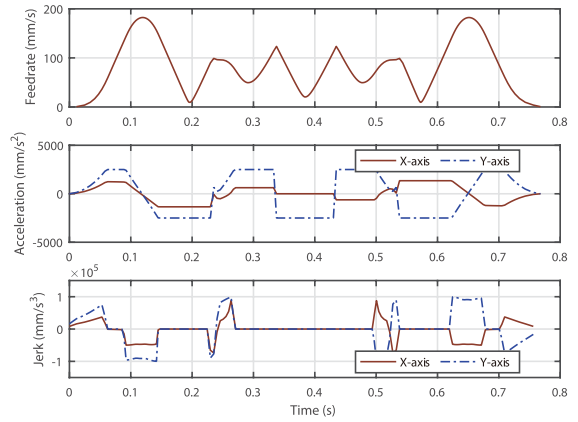


FIGURE 8. The profiles of feedrate, acceleration, jerk (the maximum jerk equals to 100000mm/s^3) for the trident path.

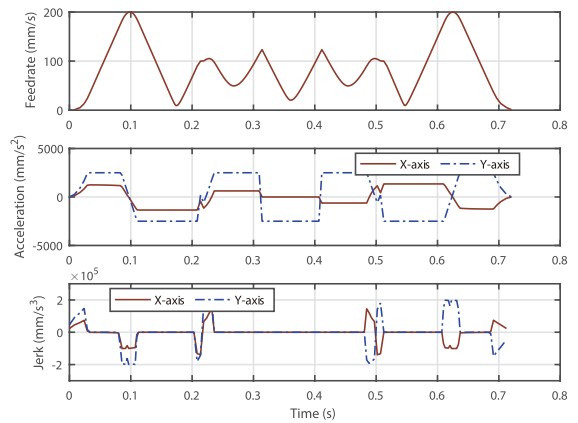


FIGURE 9. The profiles of feedrate, acceleration, jerk (the maximum jerk equals to 200000mm/s^3) for the trident path.

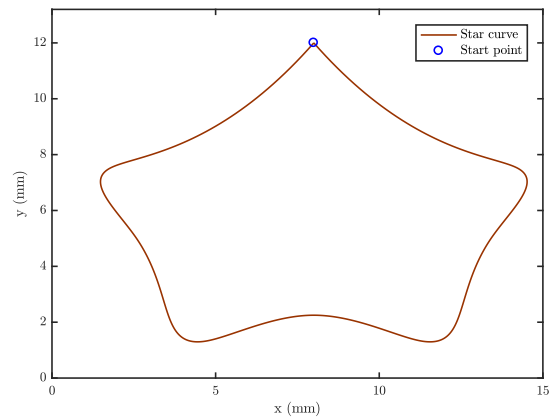


FIGURE 10. A star pattern.

in Fig.6 is chosen as the tested tool path. The parameters of the trident contour are given as follows:

$$\text{Control points: } \begin{bmatrix} 10 & 20 & 12 & 10 & 8 & 0 & 10 \\ 0 & 20 & 8 & 20 & 8 & 20 & 0 \end{bmatrix} \text{ (mm).}$$

$$\text{Weights: } W = [1, 1, 1, 1, 1, 1, 1].$$

$$\text{Knot vectors: } U = [0, 0, 0, 0.2, 0.4, 0.6, 0.8, 1, 1, 1].$$

To fully evaluate our proposed method, a different acceleration bound (2500mm/s^2) from that in section IV-A

TABLE 1. The machining time, planning time, tracking errors and contour errors under low jerk, medium jerk and high jerk bounds for trident contour.

Jerk bound	Planning time	Machining time	Tracking errors (mm)				Contour errors (mm)		Meshes
			Maximum		Mean		Maximum	Mean	
			X-axis	Y-axis	X-axis	Y-axis			
low jerk	4.568s	0.842s	0.104	0.161	0.035	0.040	0.109	0.037	571
medium jerk	4.640s	0.767s	0.151	0.207	0.062	0.081	0.146	0.040	580
high jerk	4.792s	0.721s	0.230	0.322	0.095	0.105	0.299	0.062	599

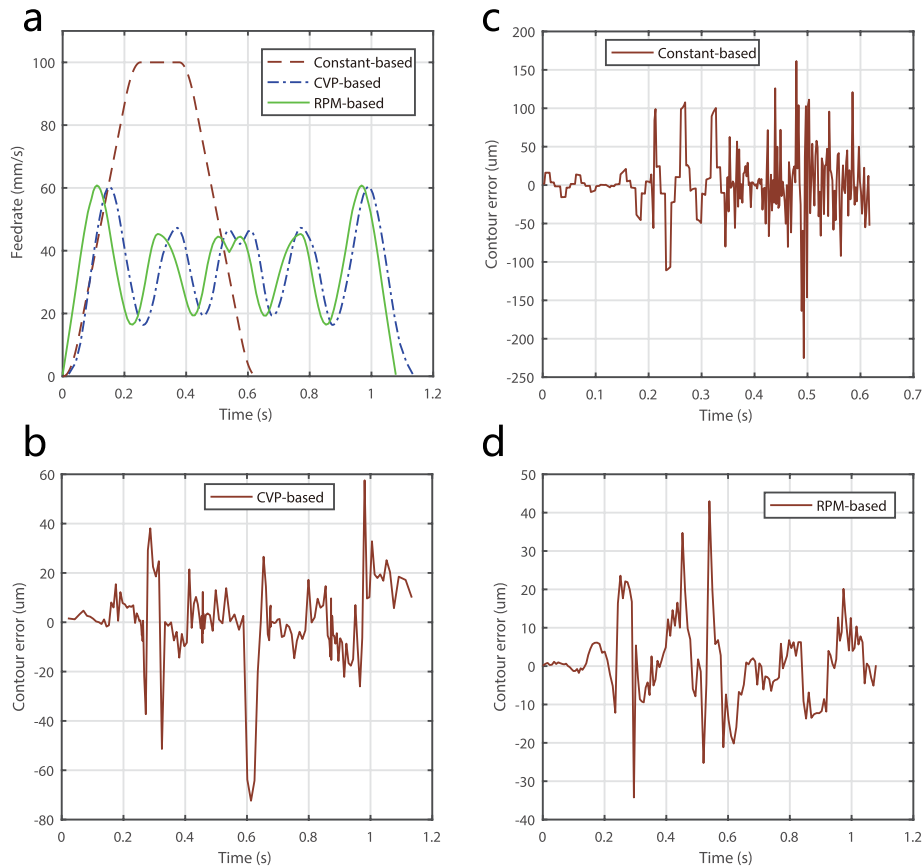


FIGURE 11. Profiles of feedrate and contour error for machining star pattern: (a) Feedrate profiles of three methods; (b) Contour error for the constant-based method; (c) Contour error for the CVP-based method; (d) Contour error for the RPM-based method.

is used. For the same reason, three different jerk bounds: the low jerk ($50000mm/s^3$), the medium jerk ($100000mm/s^3$) and the high jerk ($200000mm/s^3$), are adopted. The feedrate limit is set as $200mm/s$. The profiles of feedrate, axial acceleration and axial jerk are shown in Fig.7, when the jerk bound is set as low jerk. The profiles constrained by the medium jerk and the high jerk are drawn in Fig.8 and Fig.9. From Figs.7-9, the constraint structure of approximate “bang-bang” can be observed, especially under the high jerk constraint. The profiles of feedrate are smooth, while the profiles of axial acceleration are continuous without sudden change. Moreover, the profiles of axial jerk are perfectly bounded. Therefore, we can confirm that the presented method is effective. In addition, tracking errors and contour errors are applied to evaluate the performance of the presented method. In order to generate real time reference positions for the closed loop controllers, the feedrate profiles

under the low jerk, the medium jerk and the high jerk are interpolated according to the method of Zhang et al. [29]. A non-specialized PID controller [30] is adopted as the tracking controller for each axis. In Table.1, more detail information is listed. As shown in the table, the planning time increases with the switch from the low jerk to the high jerk, because the feasible range of the optimal solution becomes larger. As a result, the machining time becomes shorter, while the tracking errors and contour errors becomes larger. Taking the kinematic performances with the low jerk and the high jerk for example, the processing time with the high jerk bound is 14.3% less than that with the low jerk bound, but the contour error is almost doubled. If the high jerk bound is replaced by the medium jerk bound, two indexes are 9% and 8% respectively. So the jerk constraints should be chosen based on the tradeoff between the machining time and accuracy.

C. EXAMPLE III: A STAR PATH

In order to further test our proposed method, another NURBS tool path shown in Fig.10 is taken for example. The parameters of the star contour are given as follows:

Control points:

$$\begin{bmatrix} 8 & 5 & 0 & 4 & 3 & 8 & 13 & 12 & 16 & 11 & 8 \\ 12 & 8 & 8 & 4 & 0 & 3 & 0 & 4 & 8 & 8 & 12 \end{bmatrix} \text{ (mm).}$$

Weights: $W = [1, 1, 1, 1, 1, 1, 1, 1, 1, 1, 1]$.

Knot vectors:

$$U = [0, 0, 0, 0, 0.1, 0.2, 0.4, 0.5, 0.6, 0.8, 0.9, 1, 1, 1, 1].$$

The feedrate of the star path is scheduled with three different ways: constant based feed, radau-pseudo-spectral (RPM) based feed, and control vector parameterized (CVP) based feed [13]. The constant feed (dashed line) is composed of seven stages, i.e. bell-shape profile. The RPM based feed (solid line) is planned with our proposed method in section III. The CVP based feed (dash-dotted line) is also obtained through solving optimal control problems. Being different with our method, the CVP based method transforms optimal control problems into nonlinear programming problems with control vector parameterized method. Three feedrate profiles are all constrained by feed bound (100mm/s), acceleration bound (500mm/s^2), and jerk bound (20000mm/s^3). For comparison, the discrete meshes of the RPM based method and the CVP based method are set as 151.

As shown in Fig.11a, the constant based profile takes shortest cycle time which is 0.626s. It is because that once the feed bound is reached, the tool tip will cruise at that speed, neglecting geometric features of the processed path. That's why constant based feedrate leads to larger contour errors shown in Fig.11b than two other methods. The CVP based method and proposed RPM based method have almost the same cycle time, i.e. 1.133s and 1.079s. By observing Figs.11c-11d, contour errors of two optimal control based methods are of no big difference. But on the whole, the RPM based method has better performance than the CVP based method. We attribute the reason to the fact that different functions are adopted to discretize optimal control problems. The RPM based method employs the smoother lagrange polynomial rather than the piecewise constant in the CVP based method.

The maximum contour error of the RPM based method is $42.9\mu\text{m}$, whereas that of the constant based method is $161.4\mu\text{m}$. Although the constant based method saves 42% cycle time than the RPM based method, its maximum contour error is 2.8 times larger than that of the RPM based method.

V. CONCLUSION

The problem of smooth trajectory generation (PSTG) for a 3-axis machining tool can be formulated as an optimal control problem with free final time. Axial jerk constraints are adopted to smooth the feedrate profile, which can lead to a non-convex optimal control problem. In this article, to improve the computation efficiency, the pseudo

jerk constraints are employed to approximate the real jerk constraints, and therefore the non-convex optimal control problem can be replaced with the convex one. Meanwhile, the PSTG is divided into two sub-problems: PMTTP and PPSTG. The radau-pseudo-spectral method is introduced to transform sub-problems into nonlinear linear programming problems. And we propose corresponding algorithm to solve PMTTP and PPSTG. Three examples are employed to test our proposed method. Simulation results show that our method can generate smooth feedrate profile and continuous acceleration profiles. Comparing to the constant based feed, the feedrate generated by the proposed method can reduce the contour error. And the proposed RPM based method exhibits a little better performances than the CVP based method. Moreover, with our method, the approximate "bang-bang" structure of constraints are obtained. So the presented is effective.

REFERENCES

- [1] M. A. Funes-Lora, E. A. Portilla-Flores, E. Vega-Alvarado, R. R. Blas, E. A. M. Cruz, and M. F. Carbajal Romero, "A novel mesh following technique based on a non-approximant surface reconstruction for industrial robotic path generation," *IEEE Access*, vol. 7, pp. 22807–22817, 2019, doi: [10.1109/ACCESS.2019.2897079](https://doi.org/10.1109/ACCESS.2019.2897079).
- [2] M. Liu, Y. Huang, L. Yin, J. Guo, X. Shao, and G. Zhang, "Development and implementation of a NURBS interpolator with smooth feedrate scheduling for CNC machine tools," *Int. J. Mach. Tools Manuf.*, vol. 87, pp. 1–15, Dec. 2014, doi: [10.1016/j.ijmactools.2014.07.002](https://doi.org/10.1016/j.ijmactools.2014.07.002).
- [3] M. Sekar and Y. S. Han, "Design and implementation of high-performance real-time free-form NURBS interpolator in micro CNC machine tool," *Mech. Based Des. Struct. Mach.*, vol. 42, no. 3, pp. 296–311, Jul. 2014, doi: [10.1080/15397734.2014.899153](https://doi.org/10.1080/15397734.2014.899153).
- [4] L. Rutkowski, A. Przybyl, and K. Cpalka, "Novel online speed profile generation for industrial machine tool based on flexible neuro-fuzzy approximation," *IEEE Trans. Ind. Electron.*, vol. 59, no. 2, pp. 1238–1247, Feb. 2012, doi: [10.1109/TIE.2011.2161652](https://doi.org/10.1109/TIE.2011.2161652).
- [5] M. Elbanhawi and M. Simic, "Sampling-based robot motion planning: A review," *IEEE Access*, vol. 2, pp. 56–77, 2014, doi: [10.1109/ACCESS.2014.2302442](https://doi.org/10.1109/ACCESS.2014.2302442).
- [6] C. Ji, M. Kong, and R. Li, "Time-energy optimal trajectory planning for variable stiffness actuated robot," *IEEE Access*, vol. 7, pp. 14366–14377, 2019, doi: [10.1109/ACCESS.2019.2891663](https://doi.org/10.1109/ACCESS.2019.2891663).
- [7] B. Fernandez, P. J. Herrera, and J. A. Cerrada, "A simplified optimal path following controller for an agricultural skid-steering robot," *IEEE Access*, vol. 7, pp. 95932–95940, 2019, doi: [10.1109/ACCESS.2019.2929022](https://doi.org/10.1109/ACCESS.2019.2929022).
- [8] Y. Zhang, P. Ye, H. Zhang, and M. Zhao, "A local and analytical curvature-smooth method with jerk-continuous feedrate scheduling along linear toolpath," *Int. J. Precis. Eng. Manuf.*, vol. 19, no. 10, pp. 1529–1538, Oct. 2018, doi: [10.1007/s12541-018-0180-2](https://doi.org/10.1007/s12541-018-0180-2).
- [9] K. Zhang, C.-M. Yuan, X.-S. Gao, and H. Li, "A greedy algorithm for feedrate planning of CNC machines along curved tool paths with confined jerk," *Robot. Comput.-Integr. Manuf.*, vol. 28, no. 4, pp. 472–483, Aug. 2012, doi: [10.1016/j.rcim.2012.02.006](https://doi.org/10.1016/j.rcim.2012.02.006).
- [10] B. Sencer, Y. Altintas, and E. Croft, "Feed optimization for five-axis CNC machine tools with drive constraints," *Int. J. Mach. Tools Manuf.*, vol. 48, nos. 7–8, pp. 733–745, Jun. 2008, doi: [10.1016/j.ijmactools.2008.01.002](https://doi.org/10.1016/j.ijmactools.2008.01.002).
- [11] S. D. Timar and R. T. Farouki, "Time-optimal traversal of curved paths by Cartesian CNC machines under both constant and speed-dependent axis acceleration bounds," *Robot. Comput.-Integr. Manuf.*, vol. 23, no. 5, pp. 563–579, Oct. 2007, doi: [10.1016/j.rcim.2006.07.002](https://doi.org/10.1016/j.rcim.2006.07.002).
- [12] J. Mattmüller and D. Gislser, "Calculating a near time-optimal jerk-constrained trajectory along a specified smooth path," *Int. J. Adv. Manuf. Technol.*, vol. 45, nos. 9–10, p. 1007, 2009, doi: [10.1007/s00170-009-2032-9](https://doi.org/10.1007/s00170-009-2032-9).
- [13] Q. Zhang, S. Li, and J. Guo, "Smooth time-optimal tool trajectory generation for CNC manufacturing systems," *J. Manuf. Syst.*, vol. 31, no. 3, pp. 280–287, Jul. 2012, doi: [10.1016/j.jmsy.2012.06.001](https://doi.org/10.1016/j.jmsy.2012.06.001).

- [14] M. Duan and C. Okwudire, "Minimum-time cornering for CNC machines using an optimal control method with NURBS parameterization," *Int. J. Adv. Manuf. Technol.*, vol. 85, nos. 5–8, pp. 1405–1418, 2016, doi: 10.1007/s00170-015-7969-2.
- [15] F. Lin, L.-Y. Shen, C.-M. Yuan, and Z. Mi, "Certified space curve fitting and trajectory planning for CNC machining with cubic B-splines," *Comput.-Aided Des.*, vol. 106, pp. 13–29, Jan. 2019, doi: 10.1016/j.cad.2018.08.001.
- [16] Q. Gong, L. R. Lewis, and I. M. Ross, "Pseudospectral motion planning for autonomous vehicles," *J. Guid., Control, Dyn.*, vol. 32, no. 3, pp. 1039–1045, May 2009, doi: 10.2514/1.39697.
- [17] A. Gardi, R. Sabatini, S. Ramasamy, and T. Kistan, "Real-time UAS guidance for continuous curved GNSS approaches," *J. Intell. Robot. Syst.*, vol. 93, nos. 1–2, pp. 151–162, Feb. 2019, doi: 10.1007/s10846-018-0876-7.
- [18] J. Yuan, "Hierarchical motion planning for multisteering tractor-trailer mobile robots with on-axle hitching," *IEEE/ASME Trans. Mechatronics*, vol. 22, no. 4, pp. 1652–1662, Aug. 2017, doi: 10.1109/TMECH.2017.2695651.
- [19] Q. Zhang and X.-S. Gao, "Practical feedrate optimization for planar high precision contouring," in *Proc. IEEE Int. Conf. Inf. Automat. (ICIA)*, Ningbo, China, Aug. 2016, pp. 1872–1877, doi: 10.1109/ICInfA.2016.7832124.
- [20] J.-X. Guo, K. Zhang, Q. Zhang, and X.-S. Gao, "Efficient time-optimal feedrate planning under dynamic constraints for a high-order CNC servo system," *Comput.-Aided Des.*, vol. 45, no. 12, pp. 1538–1546, Dec. 2013, doi: 10.1016/j.cad.2013.07.002.
- [21] Q. Zhang, S.-R. Li, and X.-S. Gao, "Practical smooth minimum time trajectory planning for path following robotic manipulators," in *Proc. Amer. Control Conf.*, Jun. 2013, pp. 2778–2783, doi: 10.1109/ACC.2013.6580255.
- [22] J. Dong, P. M. Ferreira, and J. A. Stori, "Feed-rate optimization with jerk constraints for generating minimum-time trajectories," *Int. J. Mach. Tools Manuf.*, vol. 47, nos. 12–13, pp. 1941–1955, Oct. 2007, doi: 10.1016/j.ijmactools.2007.03.006.
- [23] Q. Zhang, S. Li, and J. Guo, "Minimum time trajectory optimization of CNC machining with tracking error constraints," *Abstract Appl. Anal.*, vol. 2014, pp. 1–15, Jan. 2014.
- [24] D. Garg, W. W. Hager, and A. V. Rao, "Pseudospectral methods for solving infinite-horizon optimal control problems," *Automatica*, vol. 47, no. 4, pp. 829–837, Apr. 2011, doi: 10.1016/j.automatica.2011.01.085.
- [25] A. Rao, D. Benson, C. L. Darby, C. Francolin, M. Patterson, I. Sanders, and G. Huntington, "Algorithm 902: Gpops, a MATLAB software for solving multiple-phase optimal control problems," *ACM Trans. Math. Softw.*, vol. 37, no. 2, 2010, Art. no. 22, doi: 10.1142/9789814307871_0003.
- [26] D. A. Benson, G. T. Huntington, T. P. Thorvaldsen, and A. V. Rao, "Direct trajectory optimization and costate estimation via an orthogonal collocation method," *J. Guid., Control, Dyn.*, vol. 29, no. 6, pp. 1435–1440, Nov. 2006, doi: 10.2514/1.20478.
- [27] D. Garg, M. A. Patterson, C. Francolin, C. L. Darby, G. T. Huntington, W. W. Hager, and A. V. Rao, "Direct trajectory optimization and costate estimation of finite-horizon and infinite-horizon optimal control problems using a radau pseudospectral method," *Comput. Optim. Appl.*, vol. 49, no. 2, pp. 335–358, Jun. 2011, doi: 10.1007/s10589-009-9291-0.
- [28] D. Garg, M. Patterson, W. W. Hager, A. V. Rao, D. A. Benson, and G. T. Huntington, "A unified framework for the numerical solution of optimal control problems using pseudospectral methods," *Automatica*, vol. 46, no. 11, pp. 1843–1851, Nov. 2010, doi: 10.1016/j.automatica.2010.06.048.
- [29] M. Zhang, W. Yan, C. Yuan, D. Wang, and X. Gao, "Curve fitting and optimal interpolation on CNC machines based on quadratic B-splines," *Sci. China Inf. Sci.*, vol. 54, no. 7, pp. 1407–1478, 2011, doi: 10.1007/s11432-011-4237-4.
- [30] M.-S. Tsai, H.-W. Nien, and H.-T. Yau, "Development of an integrated look-ahead dynamics-based NURBS interpolator for high precision machinery," *Comput.-Aided Des.*, vol. 40, no. 5, pp. 554–566, May 2008, doi: 10.1016/j.cad.2008.01.015.



KAI ZHAO received the B.S. and M.S. degrees in control science and control engineering from the China University of Petroleum (East China), Qingdao, China, in 2007, where he is currently pursuing the Ph.D. degree with the College of Control Science and Engineering.

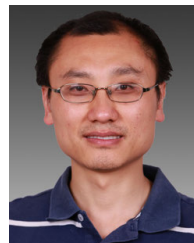
Since 2007, he has been a Lecturer with the College of Computer Science and Information Engineering, Anyang Institute of Technology. His research interests include industrial automation and intelligent robot.



ZHONGJIAN KANG received the B.S. degree from the China University of Petroleum (East China), Dongying, in 1993, and the M.S. and Ph.D. degrees in electrical engineering from the Harbin Institute of Technology, Harbin, China, in 2001.

From 2003 to 2010, he was an Assistant Professor with the China University of Petroleum (East China), where he has been a Professor with the Electrical Engineering Department, since 2010. He is the author of more than 100 articles.

His research interests include system modeling and identification, advanced control, and fault detection and diagnosis.



XIAOBO GUO received the M.S. degree from the Henan University of Science and Technology, Luoyang, China, in 2004, and the Ph.D. degree from Southeast University, Nanjing, China, in 2008.

From 2008 to 2011, he was an Associate Professor with the School of Mechanical and Power Engineering, Henan Polytechnic University, Jiaozuo, China. Since 2016, he has been a Professor with the School of Mechanical Engineering,

Anyang Institute of Technology, Anyang, China. His research interests include artificial intelligence (AI), robotics, control method, rehabilitation robot technology, and machine vision.

• • •